MRS Communications (2017), 7, 701–708

doi:10.1557/mrc.2017.60

MRS Communications

Research Letter

Poly(3,4-ethylenedioxythiophene):sulfonated poly(diphenylacetylene) complex as a hole injection material in organic light-emitting diodes

Jung Jae Kim† and **Jin Chul Yang†,** Major in Polymer Science & Engineering, School of Applied Chemical Engineering, Kyungpook National University, 80 Daehak-ro, Buk-gu, Daegu 41566, Republic of Korea
Keunbyung Yoon, Giseop Kwak, and **Jin Young Park,** Major in Polymer Science & Engineering, School of Applied Chemical Engineering, Kyungpook National University, 80 Daehak-ro, Buk-gu, Daegu 41566, Republic of Korea; Department of Polymer Science & Engineering, Kyungpook National University, 80 Daehak-ro, Buk-gu, Daegu 41566, Republic of Korea

Address all correspondence to Giseop Kwak, Jin Young Park at **gkwak@knu.ac.kr**, **jinpark@knu.ac.kr**

(Received 9 June 2017; accepted 20 July 2017)

Abstract

New ionic conjugated polyelectrolyte complex films based on poly(3,4-ethylenedioxythiophene):sulfonated poly(diphenylacetylene) (PEDOT:SPDPA) are electrochemically formed on indium thin oxide substrates using a potentiostatic method, and their physical properties are evaluated using various analytical tools. Depending on a constant applied voltage, the surface morphological features and electrochemically doped states are different due to the conformational structure related to the oxidation state in the PEDOT growth process and concomitant SPDPA doping state in the films. For the purpose of use as a hole injection layer in organic light-emitting diodes, a well-known configuration (ITP/PEDOT:SPDPA/TPD/Alq_3/LiF/Al) is adopted to investigate the optoelectronic properties.

Introduction

Conjugated polymers have attracted great interest in the field of optoelectronic devices such as organic solar cells and organic light-emitting diodes (OLEDs) owing to easier fabrication, higher flexibility, and lower manufacturing cost. In general, polyaniline and polythiophene derivatives have been widely used as hole transport layers (HTLs) in solar cells[1] or hole injection layers (HILs) in OLEDs.[2] Poly(3,4-ethylenedioxythiophene) (PEDOT) and its derivatives have also been studied extensively and used in many applications, such as tissue engineering, batteries, sensors, and corrosion protection.[3] Particularly, in the cases using as HIL or HTL materials, PEDOT is mostly used as polyelectrolyte blend systems [e.g., PEDOT:poly(styrene sulfonic acid) (PSS)].[4] Such blends are considerably useful because the energy barrier at the organic–organic interface can be adjusted by effectively controlling hole injection and transport from an active layer or anode. Furthermore, PEDOT:PSS can be synthesized either chemically or electrochemically,[5] and has been used for a long time as a HIL in OLEDs owing to its high transparency in the visible region, conductivity, and thermal stability.[6] For the optoelectronics applications, various methods have been developed to enhance the electrical conductivity of PEDOT:PSS, including solvent treatment,[7] pH adjustment,[8] electrochemical doping,[9] and use of composite layers (graphene[10] or SiO_2[11]). Moreover, other blend systems with oppositely charged polyelectrolyte materials such as poly(1-vinyl-3-ethylimidazolium),[12] poly(allylamine hydrochloride),[13] and a polystyrene backbone with (trifluoromethylsulfonyl)imide side groups,[14] instead of PSS, have recently been studied as an alternative polymer-based HIL material.

In previous study, sulfonated poly(diphenylacetylene) (SPDPA) in sodium salt form was developed and it was found that this anionic conjugated polyelectrolyte is quite emissive in visible region and highly water-soluble due to its hydrophilic sulfonate side groups in order to have an excellent ability to bind with oppositely charged molecules. Based on these unique physicochemical and fluorescence emission properties, it has recently been used in various applications such as biologic sensors, visualization of latent fingerprint, and for preparation of extremely soft conjugated polyelectrolyte–surfactant complexes.[15] In terms of viability for OLED device applications, SPDPA may offer more suitable optical features and thermal stability, and the ability to adjust the electronic properties (e.g., energy levels) for use in OLEDs will be provided as desired when combined with PEDOT. Based on this idea, we fabricated conjugated polyelectrolyte complex films consisting of PEDOT and SPDPA by electropolymerization method and examined the usefulness of the complex film as a HIL for OLEDs. The details will be described hereafter.

Experimental section

PEDOT:SPDPA thin films

SPDPA in sodium salt form was prepared according to the reference method.[15,16] To prepare the PEDOT:SPDPA films,

† These authors contributed equally to this work.

cyclic voltammetry (CV) was conducted in a three-electrode cell using a potentiostat (PARSTAT 4000, Princeton Applied Research). A clean indium-tin oxide (ITO) substrate (≈13Ω/sq.) was used as a working electrode, pretreated by successive sonication in acetone, isopropyl alcohol, and distilled ionized (DI) water for 10 min and heating at 100 °C after drying with gaseous N_2. A platinum wire and a saturated calomel electrode (SCE) were used as the counter and reference electrodes, respectively. An aqueous solution (50 mL) containing 1.8 mM (0.025 g) SPDPA was used as the supporting polymer electrolyte and 10 mM (0.07 g) 3,4-ethylenedioxythiopene (EDOT, Sigma-Aldrich Co.) was used as the electroactive monomer. The CV was performed over a scanning range of −0.8 to 1.3 V (versus SCE) at a scanning rate of 50 mV/s with five scanning cycles. To control the extent of doping in the PEDOT:SPDPA films, a potentiostatic method was used in the same aqueous solution. Various constant potentials (0.9–1.3 V versus SCE) were applied for controlled durations to obtain films of the same thickness. After thorough rinsing with DI water, the films were dried with gaseous N_2.

Characteristics

To investigate functional groups on the PEDOT:SPDPA films, the electrodeposited films at various constant voltages for 30 min were collected using a single-edge blade and mixed with KBr (1:150, w/w) to prepare a pellet. Fourier transform infrared (FTIR; FT/IR-4100, JASCO) measurements were performed over a spectral range of 600–4000 cm^{-1} at a resolution of 4 cm^{-1}. For differential scanning calorimetry (DSC) measurements (DSC Q2000, TA Instruments), the PEDOT:SPDPA compound (1 mg) was placed in a pan and heated from −50 to 250 °C at a speed of 10 °C/min. The temperature was then maintained for 2 min before cooling to −50 °C at a speed of 5 °C/min in the primary thermal cycle. In the secondary cycle, the temperature was maintained for 2 min, and then increased from −50 to 250 °C at a speed of 5 °C/min. Thermal gravimetric analysis (TGA) measurements (LABSYS evo, SETARAM Instrumentation) were performed by heating each different PEDOT:SPDPA and SPDPA (6–12 mg) over a temperature range (50–575 °C) at a speed of 5 °C/min after drying in a vacuum oven. Atomic force microscopy (AFM; NX20, Park Systems) and scanning electron microscopy (SEM) images (S-4800, Hitachi High-Technology) were obtained to investigate surface morphological features of electrodeposited PEDOT:SPDPA films. A COH-400 spectrophotometer (Nippon Denshoku) was used to measure the color. To measure the highest occupied molecular orbital (HOMO) and lowest unoccupied molecular orbital (LUMO) energy levels, the following procedure was implemented. First, to measure the half-wave potential of ferrocene (Fc), CV was performed in an acetonitrile solution with Fc (10 mM) and $LiClO_4$ (0.1 M; Sigma-Aldrich Co.) over a scan range of 0–0.6 V at a scan rate of 0.1 V/s. Next, using each PEDOT:SPDPA film electrodeposited on a milli-electrode (G0228, Ametek) at various constant voltages, CV was performed in an acetonitrile solution with $LiClO_4$ (0.1 M) at a scan range of −0.8 to 1.3 V and a scan rate of 0.1 V/s.

Device fabrication and evaluation

For OLED device fabrication, the followings were used: N,N′-bis(3-methylphenyl)-N,N′-diphenylbenzidine (TPD; Luminescence Technology Corporation, Taiwan) as a HTL, tris(8-hydroxyquinolinato)aluminum (Alq_3; Toyo Ink, Japan) as an emitting layer, aluminum (Al; High Purity Chemicals Laboratory, Japan) and lithium fluoride (LiF, Sigma-Aldrich Co.) as a cathode, and ITO glass (13 Ω/sq., transmission 88%) as an anode. Several SPDPA-doped PEDOT compiles films with an identical thickness of 50 nm were prepared by electrodeposition in an aqueous solution with EDOT (10 mM) and SPDPA (10 mM) at a constant applied voltage in the range of 0.9–1.3 V. After drying all the films, TPD (60 nm, 1 Å/s) and Alq_3 (40 nm, 1 Å/s) were sequentially evaporated on the HIL/ITO substrates through a shadow mask under high vacuum ($<5.0 \times 10^{-7}$ Torr) using a cluster-type metal/organic material sputtering system (EL+200, Sunic System Co., Ltd.). As a cathode for the devices, Al (120 nm, 1 Å/s) was sublimated under the same conditions. To evaluate the device performance, all parameters were measured using an IVL (current–voltage–luminance) testing system (PR650, Photoresearch SpectraScan) under an applied voltage range of 0–12 V in a 0.5 V interval over an emitting area of 9 cm^2.

Results and discussion

Similar to the electrochemical polymerization of other electroactive monomers (e.g., pyrrole and aniline), subjecting the SPDPA polyelectrolyte to CV facilitates the formation of PEDOT:SPDPA thin films [chemical structure in Fig. 1(a)] on ITO substrates through ionic interaction. As shown in the cyclic voltammogram [Fig. 1(b)], the onset voltage of the anodic current is observed at approximately 0.82 V (versus SCE), reflecting the formation of the radical cations. In each scan, the current increase as the potential becomes more positive. In addition, both the anodic and cathodic waves grow upon continuous cycling (five cycles), which indicates that the thickness of the conductive polymeric film is increasing. During the electrochemical oxidation process, both EDOT monomers/oligomers in solution and other polymer chains on the film continuously react and oxidize, forming longer chains through coupling reactions at the 2,6 position. In this process, the conjugation structure of the chains (oligomers or polymers) is stabilized in oxidized form on the film, interacting with SPDPA as a charge-balancing dopant. Based on the electrochemical behaviors of the film formation revealed by CV, potentiostatic polymerization was performed to maintain a highly oxidative state on the PEDOT chains. Applying a higher potential than the onset voltage increases the chain length as a result of the simultaneous occurrence of the coupling reaction of the monomers and ionic interaction of the oxidized polymer (positively charged backbone) with the anionic polyelectrolyte. This deposition enables the formation of PEDOT:SPDPA films with doping-generated polarons in a conductive state.

Five different SPDPA-doped PEDOT films with almost identical thicknesses were prepared by applying a specific

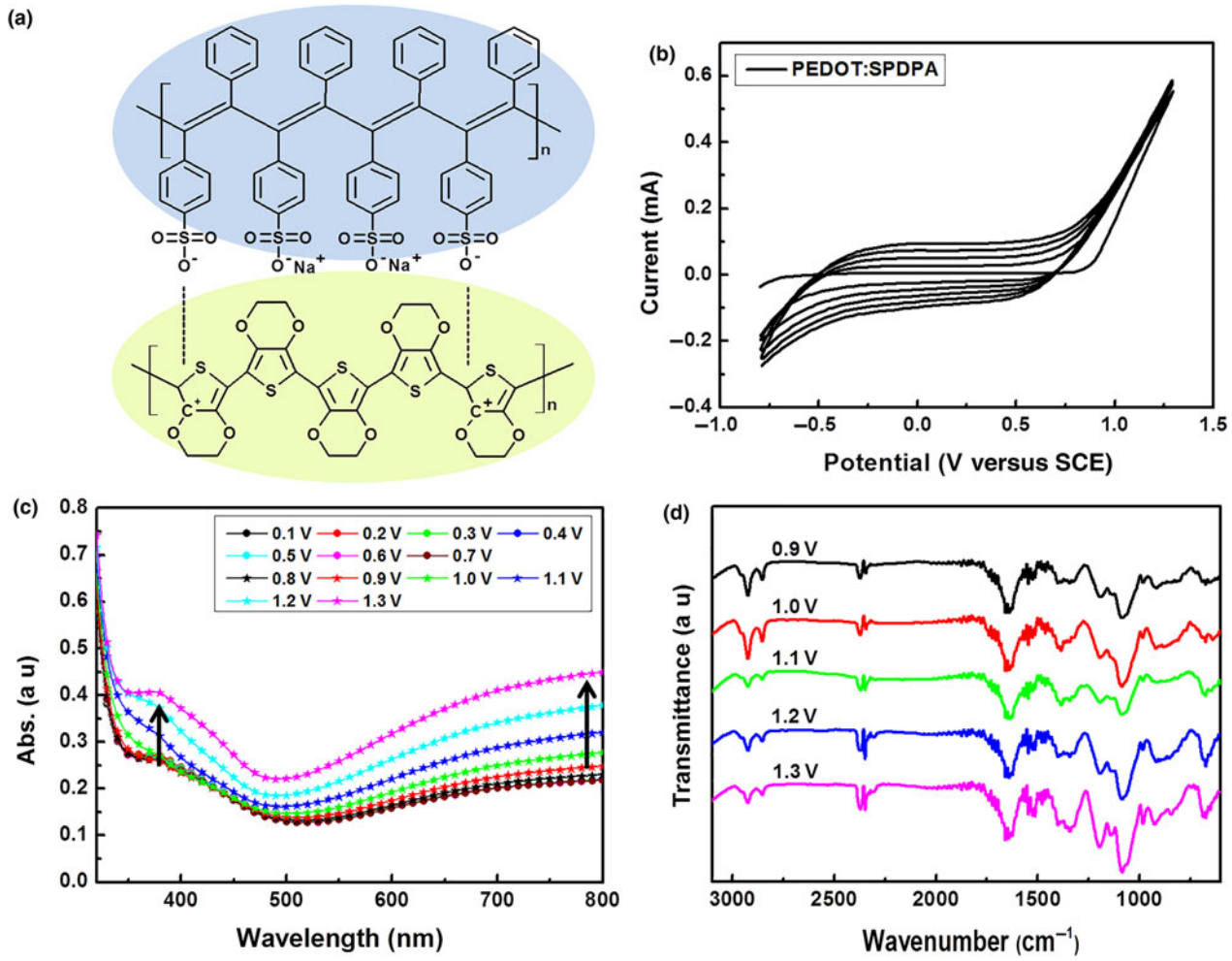

Figure 1. (a) Chemical structures of PEDOT:SPDPA composite with ionic interactions, (b) CV voltammograms of PEDOT:SPDPA in an aqueous solution with 10 mM EDOT and 1.8 mM SPDPA (voltage range: −0.8 to1.3 V, scan rate: 0.05 V/s, 5 sweep cycles), (c) change in absorbance of the PEDOT:SPDPA film (sample preparation: CV) with the degree of PEDOT polarons/bipolarons formed by electrochemical doping (applying constant voltage for 60 s), and (d) FTIR spectra of PEDOT:SPDPA films potentiostatically polymerized under each constant voltages within a range of 0.9 and 1.3 V.

constant potential in the range of 0.9–1.3 V for a controlled deposition time. During film formation, positively charged PEDOT and negatively charged SPDPA underwent ionic complexation depending on the charge balance of the two components. As observed in the ultraviolet–visible (UV–vis) absorption and photoluminescence (PL) emission spectra (Fig. S1), SPDPA had two absorption peaks at 379 and 438 nm. On the other hand, the PEDOT:SPDPA films showed a broad band between 550 and 800 nm together with a peak at 378 nm. The broad band resulted from the $\pi - \pi^*$ absorption transition in the oxidized polymer matrix, similar to the cases of PEDOT:PSS or electropolymerized PEDOT.[17] The SPDPA exhibited a significant PL maximum at 540 nm, whereas the PL was almost quenched in the PEDOT:SPDPA films owing to the intermolecular $\pi - \pi$ interaction upon formation of a stable ionomer complex between PEDOT and SPDPA.[18] To identify the effects of the doping state on the absorption properties, based on spectroelectrochemistry the ex situ UV–vis spectra of the PEDOT:SPDPA film [initially made by the CV method as shown in Fig. 1(b)] were investigated by applying 0.1 V for 60 s, and then collecting optical data. Thereafter, the same film on which a stepwisely increased constant voltage was applied up to 1.3 V (voltage interval: 0.1 V) was also repeatedly measured in the same way. As shown in Fig. 1(c), above 0.9 V, a distinct, broad absorption band appears at 500–800 nm due to the formation of the polaron and bipolaron subgap states from the heavily doped nature of the film, and an increase in the peak intensity at 378 nm is observed upon oxidation.[19] To characterize the two components in PEDOT:SPDPA films, FTIR spectra were recorded [Fig. 1(d)]. Regardless of the electrochemical deposition conditions, similar functional group vibrations are observed in all

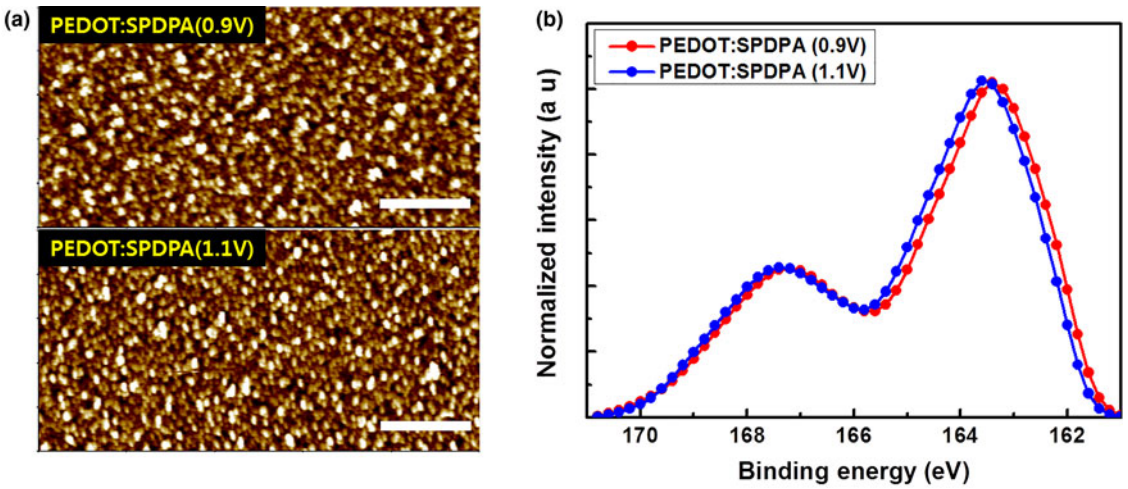

Figure 2. (a) AFM images of PEDOT:SPDPA films deposited at constant potentials of 0.9 and 1.1 V (scale bars: 1 μm) and (b) XPS *S*(2*p*) spectra of PEDOT:SPDPA films fabricated at constant voltages of 0.9 and 1.1 V.

the spectra. The absorption peak at 1194 cm^{-1} is assigned to sulfonate groups in SPDPA, while the two peaks at 2852 and 2926 cm^{-1} are assigned to ethylene moieties in PEDOT.[14] The fingerprint-region peaks at 1084, 983, and 842 cm^{-1} originate from PEDOT.[20]

As shown in the AFM images [Fig. 2(a)], under a relatively low applied potential (0.9 V), the surface of PEDOT:SPDPA film was somewhat rough (root-mean-square roughness, R_q = 6.50 nm). However, at an applied potential of 1.1 V, the film structure was quite dense and relatively well distributed (R_q = 5.60 nm). This variation in the surface morphology was found to be determined by the electrochemical growth behaviors of PEDOT:SPDPA depending on applied potential. For further insights into the composition ratio, the X-ray photoelectron spectroscopy (XPS) spectra of the PEDOT:SPDPA films prepared at applied voltages of 0.9 and 1.1 V were compared [Fig. 2(b)]. In both films, *S*(2*p*) peaks from the sulfonate of SPDPA and thiophene of PEDOT appear at binding energies of 167.3 and 163.5 eV, respectively,[21] and the surface intensity ratios of SPDPA to PEDOT are 1:2.252 and 1:2.247, respectively. In general, commercial PEDOT:PSS, in which PEDOT particles are formed with insulating PSS domains shows the higher sulfur signal from sulfonate of PSS than that in thiophene of PEDOT.[22] However, in the case of the electrochemical approach for PEDOT:SPDPA ionic complexation the SPDPA content represents almost half-reduced binding energy, rather than the sulfur signal in PEDOT.

As shown in Fig. 3 (DSC and TGA), the thermal properties of PEDOT:SPDPA were investigated to evaluate its viability as a HIL in optoelectronics in terms of thermal stability. In the DSC curves, the complex powder has no significant peak related to glass transition temperature. During the first heating scan, an endothermic peak due to the melting of small PEDOT:SPDPA crystals appears at 73 °C, while the same peak appears at approximately 90–110 °C in PEDOT:PSS.[23] During the second scan, however, no peak is observed. This indicates that the PEDOT:SPDPA powder did not undergo any phase transition such as crystallization or melting during the first cooling process. The TGA of PEDOT:SPDPA and SPDPA was performed. The PEDOT:SPDPA showed the first mass loss (10–15%) in the temperature range of 160–285 °C, and the mass loss of the electrodeposited materials at 280 °C varies slightly with the degree of oligomer formation under the driving force of electrodeposition (constant applied potential). At much higher temperatures (285–345 °C), a similar mass loss (20%) was observed for all electrodeposited PEDOT:SPDPA probably due to the decomposition of sulfonate groups on SPDPA.[24] The mass loss associated with the degradation of the PEDOT and SPDPA backbones was seen above 345 °C. The TGA results indicate that each composite material contains the same mass of SPDPA.

Prior to the fabrication and characterization of OLED devices using the PEDOT:SPDPA films as HILs, the HOMO and LUMO energy levels were first calculated from the CVs on the basis of the onset points of the redox curves and half-potential of Fc (Fig. S2).[25] All the electrodeposited PEDOT:SPDPA films have almost identical low bandgaps (1.37–1.4 eV), and the HOMO (5.42–5.45 eV) and LUMO (4.02–4.08 eV) energy levels were calculated [Fig. 4(a)]. The change in energy levels does not differ significantly among the films, but is highly different from the values for PEDOT:PSS (HOMO, 5.2 eV; LUMO, 2.3 eV). Accordingly, hole injection from the ITO anode is much easier than that in PEDOT:PSS due to the lower HOMO level in the PEDOT:SPDPA film. In addition, their low bandgap (near-IR absorption, typically $E_g < 1.6$ eV) suggests their potential use in device applications, such as organic photovoltaics (OPV) and field-effect transistors (FETs).[26] The surface morphological

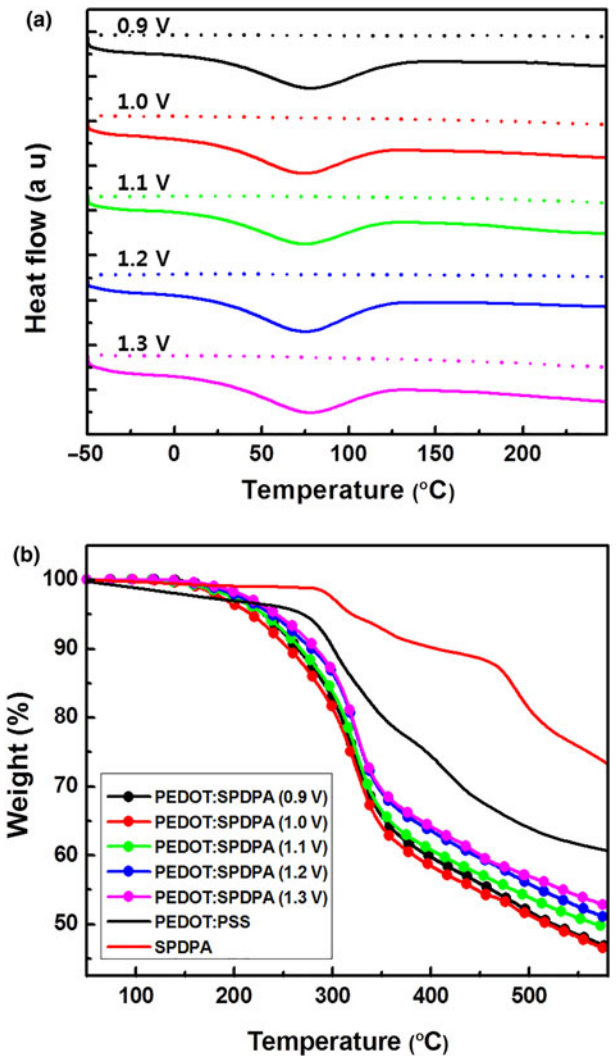

Figure 3. (a) DSC and (b) TGA measurements of each PEDOT:SPDPA fabricated by inducing constant voltage in the range of 0.9–1.3 V. In DSC measurements, the solid and dashed lines correspond to the first and second heating, respectively. TGA measurements include the results for SPDPA.

features differ significantly depending on the conformational structure related to the oxidation state in the PEDOT growth process and concomitant SPDPA doping state in the films (Fig. S3). At applied potentials of 0.9 and 1.0 V, rough, porous films are formed. However, the film obtained at an applied potential of 1.1 V is obviously smoother. Furthermore, at the higher applied voltage (1.2 and 1.3 V), the film surfaces feature many bumps due to the strong electrochemical driving force induced during the PEDOT:SPDPA film formation. Thus, the electrochemical conditions for the film formation may determine the PEDOT oxidation state and its ionic complexation with SPDPA during polymerization.

Based on the film characteristics described previously, OLEDs were fabricated onto SPDPA-doped PEDOT films. Five PEDOT:SPDPA films with an identical thickness of 50 nm on ITO substrates were fabricated under different electrochemical conditions and used as HILs with TPD and Alq_3 used as the hole transport and emitting layers, respectively. All devices show the same turn-on voltage ($V_T = 3.2$ V), whereas the OLED with PEDOT:SPDPA (1.1 V) film has the highest current density at a given voltage, indicating that hole injection is more efficient on the interface due to the difference in the morphology formed in the electrochemical deposition [Fig. 4(b)]. This device presents the highest maximum brightness ($B_{max} = 202$ cd/m^2 at 7.5 V) among the electrodeposited films [Fig. 4(c)]. In addition, when applying potential up to 1.1 V for film formation, other device performance properties, such as the electroluminescence (EL) efficiency and external quantum efficiency, are increased. In contrast, higher applied potentials (>1.2 V) significantly degrade the device performance properties as a result of an overoxidation process that generally occurs under an anodic overpotential due to the presence of water or oxygen, deactivating the conductivity in PEDOT.[27] As a result, the poor intrinsic hole transport in the film, which is related to the conformational structure upon ionic polymer complexation, causes poor device performance. Consequently, the PEDOT:SPDPA film (1.1 V) showed the highest maximum EL efficiency (0.59 cd/A) at relatively low device voltage (4 V) because of much efficient hole injection, associated with structural formation. All the devices exhibit typical green light-emitting characteristics with an EL peak in the range of 519–521 nm and $x = 0.30$ and $y = 0.54$ in CIE coordinates [Fig. 4(d)]. Table I summarizes the device performance of the green OLEDs with electrodeposited PEDOT:SPDPA films as HILs. For comparison with the devices with PEDOT:SPDPA HILs, OLEDs without an HIL were investigated. The no-HIL OLED shows more dramatically enhanced emission properties ($B_{max} = 527$ cd/m^2), albeit with a slightly higher VT (4.5 V). This is because of the absence of negative effects, such as poor intrinsic film properties and even the 5–7% relative transmittance loss (based on ITO, with a transmittance of 89.63%) of the PEDOT:SPDPA or commercial PEDOT:PSS film at a wavelength of 520 nm (Fig. S4).

To enhance the EL emission properties, OLEDs with an additional LiF buffer layer (≈1 nm, 0.1 Å/s) and thermal annealing (150 °C, 20 min) were investigated (Fig. 5). A buffer layer that is thermally evaporated onto PEDOT:SPDPA(1.1 V)/TPD/Alq_3 layers generally decreases the work function of an Al cathode down to 3.5 eV, improving electron injection into the emitting layer.[28] In this case, the Bmax of 1552 cd/m^2 is dramatically enhanced, being almost eight orders of magnitude higher than that of OLED without a LiF layer, and the other device performance parameters are also slightly improved. In addition to the LiF layers, thermal annealing also significantly influences the device performance due to a conformational change induced by film shrinkage.[29] The V_T of the annealed PEDOT:SPDPA device (3 V) is lower than that of the device not subjected to thermal treatment ($V_T = 3.3$ V). The enhanced B_{max} of 3235 cd/m^2 at 6.5 V is observed due to the rearrangement of the film conformation and loss of water, resulting in

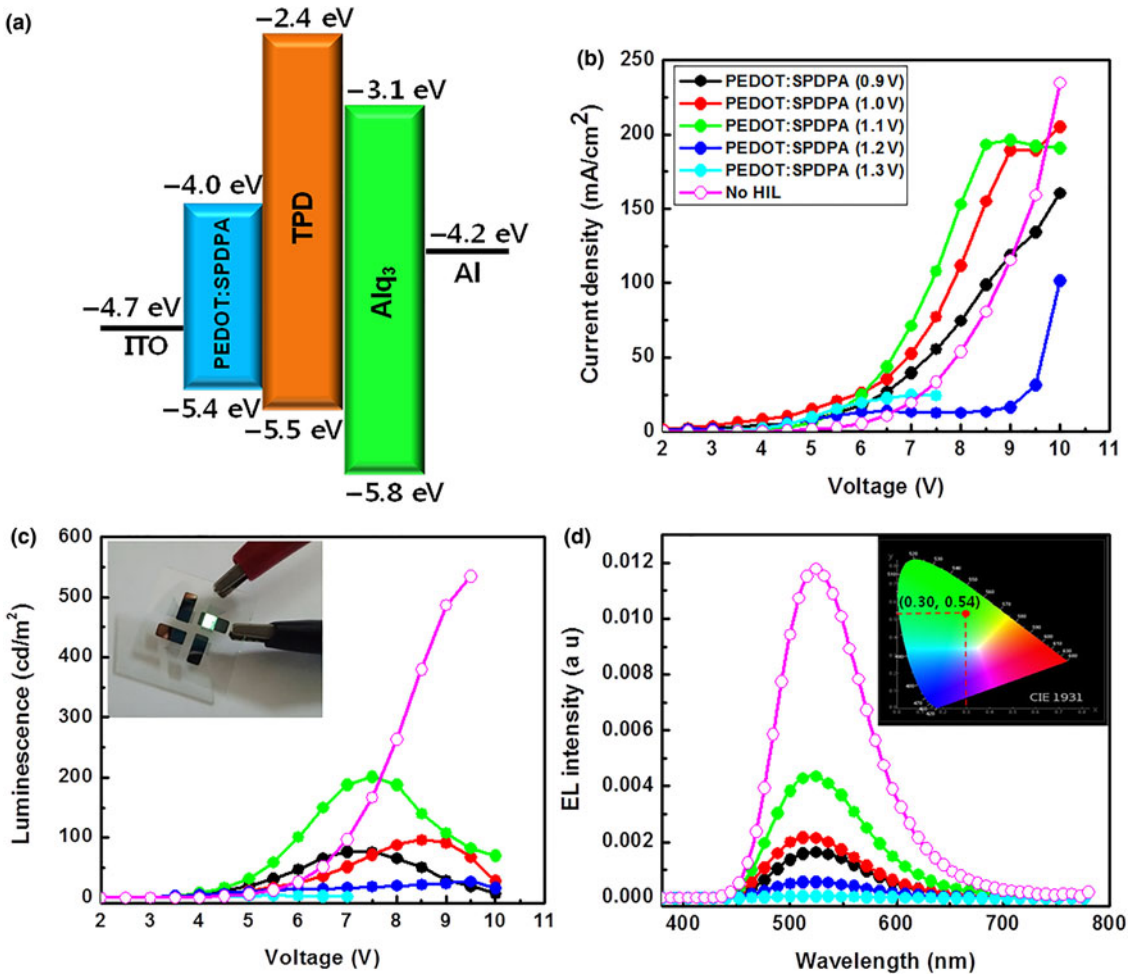

Figure 4. (a) Band structures of OLEDs: PEDOT:SPDPA/TPD/Alq_3, (b–d) Current–voltage (J–V), luminescence–voltage (L–V), and EL intensity-wavelength for OLEDs with PEDOT:SPDPA HIL films fabricated using different film preparation conditions.

improved conductivity. Compared with the PEDOT:PSS film,[30] a similar phenomenon may occur on the PEDOT:SPDPA films as the annealed films (fabricated at constant potentials of 0.9 and 1.1 V) are smoother and rearranged (R_q = 6.31 and 5.33 nm, respectively) (Fig. S5).

Conclusions

We presented electrodeposited PEDOT:SPDPA films as an alternative common HIL and characterized their thermal and optical properties depending on the electrostatic deposition conditions to evaluate their potential use in optoelectronic devices. At an

Table I. Performance parameters of devices utilizing various electrochemically deposited PEDOT:SPDPA films.

Electrochemical conditions		OLEDs				
V_{EC} (V)	t (s)	B_{max} (cd/m^2)	V_T (V)	η_A (cd/A)	η_{EQE} (%)	λ_{EL} (nm)
0.9	150	77	3.5	0.26	0.9	521
1.0	70	96	3.5	0.10	0.4	519
1.1	48	202	3.5	0.59	2.1	520
1.2	38	27	3.5	0.28	1.0	520
1.3	30	3	3.5	0.04	0.2	520

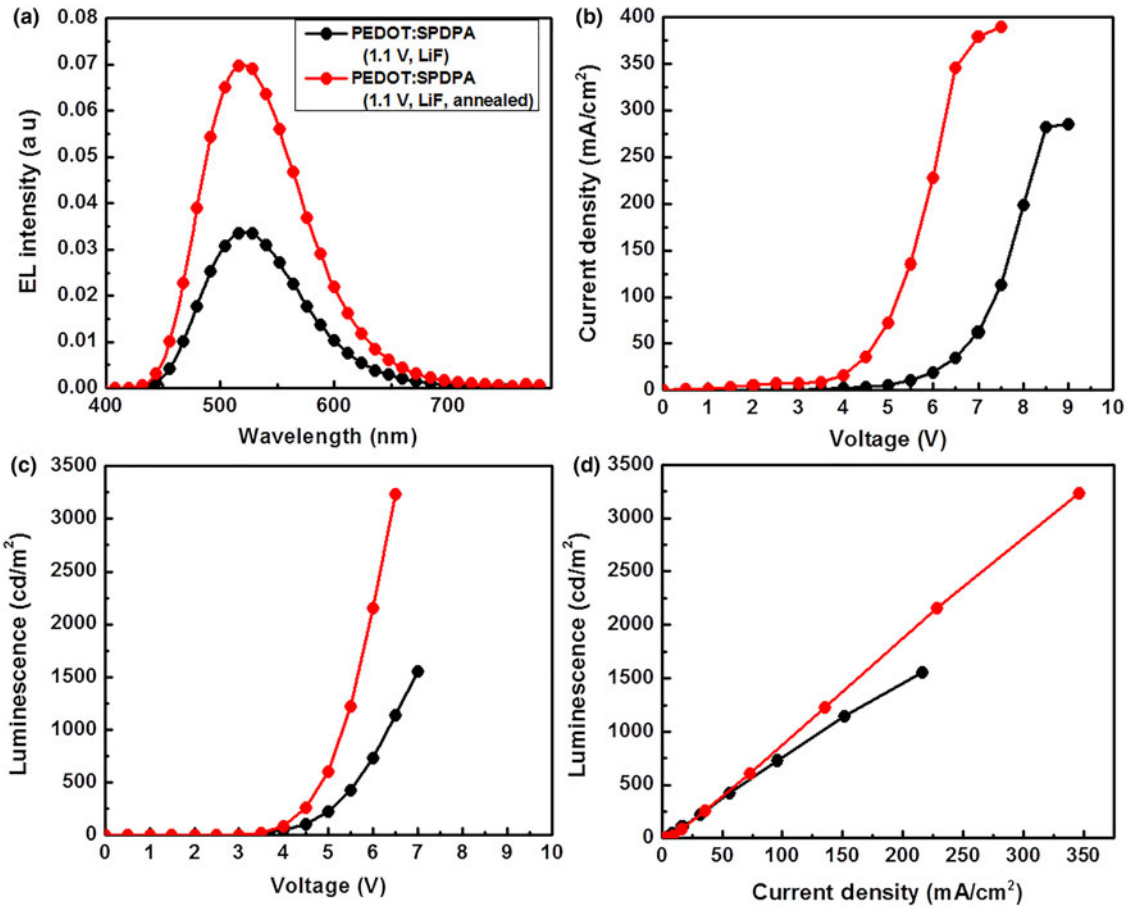

Figure 5. Use of a LiF buffer layer and thermal annealing of PEDOT:SPDPA films in OLEDs: (a) EL versus wavelength, (b) current density versus voltage, (c) luminescence versus voltage, and (d) luminescence versus current density for OLEDs using PEDOT:SPDPA as a HIL in an ITO/HIL/TPD/Alq_3/(LiF)/Al structure.

applied potential of 1.1 V, a highly smooth and organized PEDOT:SPDPA film was formed. Furthermore, all the films had similar energy levels, facilitating hole injection. Based on the characteristics of these films, we fabricated green OLEDs with various PEDOT:SPDPA films as HILs and characterized the EL properties of the devices. In terms of device performance, the optimum electrodeposition condition was found to be a constant applied potential of 1.1 V for PEDOT:SPDPA film formation. Further study on solvent treatments or device structure will improve the device performances.

Supplementary material

The supplementary material for this article can be found at https://doi.org/10.1557/mrc.2017.60.

Acknowledgments

We gratefully acknowledge financial support from the Mid-Career Science Research Program through the NRF funded by the Ministry of Science, ICT & Future Planning (NRF-2016R1A2B4010633).

References

1. K. Sun, S. Zhang, P. Li, Y. Xia, X. Zhang, D. Du, F.H. Isikgor, and J. Ouyang: Review on application of PEDOTs and PEDOT:PSS in energy conversion and storage devices. *J. Mater. Sci.: Mater. Electron.* **26**, 4438–4462 (2015).
2. H. Bejbouj, L. Vignau, J.L. Miane, T. Olinga, G. Wantz, A. Mouhsen, E.M. Oualim, and M. Harmouchi: Influence of the nature of polyaniline-based hole-injecting layer on polymer light emitting diode performances. *Mat. Sci. Eng. B: Solid* **166**, 185–189 (2010).
3. L. Groenendaal, F. Jonas, D. Freitag, H. Pielartzik, and J.R. Reynolds: Poly (3,4-ethylenedioxythiophene) and its derivatives: past, present, and future. *Adv. Mater.* **12**, 481–494 (2000).
4. H. Jiang, P. Taranekar, J.R. Reynolds, and K.S. Schanze: Conjugated polyelectrolytes: synthesis, photophysics, and applications. *Angew. Chem. Int. Ed.* **48**, 4300–4316 (2009).
5. J. Yan, C. Sun, F. Tan, X. Hu, P. Chen, S. Qu, S. Zhou, and J. Xu: Electropolymerized poly(3,4-ethylenedioxythiophene):poly(styrene sulfonate) (PEDOT:PSS) film on ITO glass and its application in photovoltaic device. *Sol. Energy Mater. Sol. Cells* **94**, 390–394 (2010).
6. S.A. Choulis, V.E. Choong, A. Patwardhan, M.K. Mathai, and F. So: Interface modification to improve hole-injection properties in organic electronic devices. *Adv. Funct. Mater.* **16**, 1075–1080 (2006).
7. N. Kim, S. Kee, S.H. Lee, B.H. Lee, Y.H. Kahng, Y.R. Jo, B.J. Kim, and K. Lee: Highly conductive PEDOT:PSS nanofibrils induced by solution-processed crystallization. *Adv. Mater.* **26**, 2268–2272 (2014).
8. M.M. de Kok, M. Buechel, S.I.E. Vulto, P. van de Weijer, E.A. Meulenkamp, S.H.P.M. de Winter, A.J.G. Mank, H.J.

M. Vorstenbosch, C.H.I. Weijtens, and V. van Elsbergen: Modification of PEDOT:PSS as hole injection layer in polymer LEDs. *Phys. Status Solidi* (*a*) **201**, 1342–1359 (2004).
9. K. Walzer, B. Maennig, M. Pfeiffer, and K. Leo: Highly Efficient organic devices based on electrically doped transport layers. *Chem. Rev.* **107**, 1233–1271 (2007).
10. J.C. Yu, J.I. Jang, B.R. Lee, G.W. Lee, J.T. Han, and M.H. Song: Highly efficient polymer-based optoelectronic devices using PEDOT:PSS and a GO composite layer as a hole transport layer. *ACS Appl. Mater. Interfaces* **6**, 2067–2073 (2014).
11. B. Riedel, Y. Shen, J. Hauss, M. Aichholz, X. Tang, U. Lemmer, and M. Gerken: Tailored highly transparent composite hole-injection layer consisting of Pedot:PSS and SiO_2 nanoparticles for efficient polymer light-emitting diodes. *Adv. Mater.* **23**, 740–745 (2011).
12. T.Y. Kim, M. Suh, S.J. Kwon, T.H. Lee, J.E. Kim, Y.J. Lee, J.H. Kim, M.P. Hong, and K.S. Suh: Poly(3,4-ethylenedioxythiophene) derived from poly(ionic liquid) for the use as hole-injecting material in organic light-emitting diodes. *Macromol. Rapid Commun.* **30**, 1477–1482 (2009).
13. C.A. Cutler, M. Bouguettaya, T.S. Kang, and J.R. Reynolds: Alkoxysulfonate-functionalized PEDOT polyelectrolyte multilayer films: electrochromic and hole transport materials. *Macromolecules* **38**, 3068–3074 (2005).
14. A.I. Hofmann, W.T.T. Smaal, M. Mumtaz, D. Katsigiannopoulos, C. Brochon, F. Schütze, O.R. Hild, E. Cloutet, and G. Hadziioannou: An alternative anionic polyelectrolyte for aqueous PEDOT dispersions: toward printable transparent electrodes. *Angew. Chem. Int. Ed.* **54**, 8506–8510 (2015).
15. W.E. Lee, Y.J. Jin, S.I. Kim, G. Kwak, J.H. Kim, T. Sakaguchi, and C. L. Lee: Fluorescence turn-on response of a conjugated polyelectrolyte with intramolecular stack structure to biomacromolecules. *Chem. Commun.* **49**, 9857–9859 (2013).
16. W.E. Lee, Y.J. Jin, B.S.I. Kim, G. Kwak, T. Sakaguchi, H.H. Lee, J.H. Kim, J.S. Park, N. Myoung, and C.L. Lee: In-situ electrostatic self-assembly of conjugated polyelectrolytes in a film. *Adv Mater Interfaces Adv. Mater. Interfaces* **1**, 1400360 (2014).
17. C. Janáky, G. Bencsik, Á. Rácz, and C. Visy: Electrochemical grafting of poly(3,4-ethylenedioxythiophene) into a titanium dioxide nanotube host network. *Langmuir* **26**, 13697–13702 (2010).
18. T. Koyama, T. Matsuno, Y. Yokoyama, and H. Kishida: Photoluminescence of poly(3,4-ethylenedioxythiophene)/poly(styrene-sulfonate) in the visible region. *J. Mater. Chem. C* **3**, 8307–8310 (2015).
19. R. Gangopadhyay, B. Das, and M.R. Molla: How does PEDOT combine with PSS? Insights from structural studies. *RSC Adv.* **4**, 43912–43920 (2014).
20. N. Sakai, G.K. Prasad, Y. Ebina, K. Takada, and T. Sasaki: Layer-by-layer assembled TiO_2 nanoparticle/PEDOT-PSS composite films for switching of electric conductivity in response to ultraviolet and visible light. *Chem. Mater.* **18**, 3596–3598 (2006).
21. X. Crispin, F.L.E. Jakobsson, A. Crispin, P.C.M. Grim, P. Andersson, A. Volodin, C. van Haesendonck, M. Van der Auweraer, W.R. Salaneck, and M. Berggren: The origin of the high conductivity of poly (3,4-ethylenedioxythiophene)−poly(styrenesulfonate) (PEDOT−PSS) plastic electrodes. *Chem. Mater.* **18**, 4354–4360 (2006).
22. Y.H. Kim, C. Sachse, M.L. Machala, C. May, L. Müller-Meskamp, and K. Leo: Highly conductive PEDOT:PSS electrode with optimized solvent and thermal post-treatment for ITO-free organic solar cells. *Adv. Funct. Mater.* **21**, 1076–1081 (2011).
23. M. Culebras, C.M. Gómez, and A. Cantarero: Thermoelectric measurements of PEDOT:PSS/expanded graphite composites. *J. Mater. Sci.* **48**, 2855–2860 (2013).
24. M. Teraguchi, and T. Masuda: Polymerization of diphenylacetylenes having very bulky silyl groups and polymer properties. *J. Polym. Sci. A: Polym. Chem.* **36**, 2721–2725 (1998).
25. G. Gritzner, and J. Kuta: Recommendations on reporting electrode potentials in nonaqueous solvents. *Pure Appl. Chem.* **56**, 461–466 (1984).
26. R.A.J. Janssen, and J. Nelson: Factors limiting device efficiency in organic photovoltaics. *Adv. Mater.* **25**, 1847–1858 (2013).
27. H.J. Ahonen, J. Lukkari, and J. Kankare: n- and p-Doped poly (3,4-ethylenedioxythiophene): two electronically conducting states of the polymer. *Macromolecules* **33**, 6787–6679 (2000).
28. H. Mu, W. Li, R. Jones, A. Steckl, and D. Klotzkin: A comparative study of electrode effects on the electrical and luminescent characteristics of Alq_3/TPD OLED: improvements due to conductive polymer (PEDOT) anode. *J. Lumin.* **126**, 225–229 (2007).
29. J. Huang, P.F. Miller, J.S. Wilson, A.J. de Mello, J.C. de Mello, and D.D. C. Bradley: Investigation of the effects of doping and post-deposition treatments on the conductivity, morphology, and work function of poly (3,4-ethylenedioxythiophene)/poly(styrene sulfonate) films. *Adv. Funct. Mater.* **15**, 290–296 (2005).
30. B. Friedel, P.E. Keivanidis, T.J.K. Brenner, A. Abrusci, C.R. McNeill, R. H. Friend, and N.C. Greenham: Effects of layer thickness and annealing of PEDOT:PSS layers in organic photodetectors. *Macromolecules* **42**, 6741–6747 (2009).